International Journal of Trend in Scientific Research and Development (IJTSRD)
Volume 5 Issue 3, March-April 2021 Available Online: www.ijtsrd.com e-ISSN: 2456 – 6470

An Analysis of Mechanical Properties and Flexural Behavior of Concrete Slabs Reinforced with H.F.R.P Reinforcements

Prerna Vaidya, Prof. Nitesh Kushwaha, Prof. Afzal Khan

Department of Civil Engineering, Millennium Institute of Technology, Bhopal, Madhya Pradesh, India

ABSTRACT

In the era of concrete, concrete is exposed to chemical, such as carbonation and chloride adulteration break down the alkaline barrier in the cement. Subsequently, steel in the concrete becomes corrosive. Such phenomena lead to erosion of concrete at the reinforcement level, cracking and spelling of concrete due to volume increase of steel reinforcement. Different methods were investigated to overcome corrosion by numerous researchers.

According to A.S.T.M D792-13 standards the density of H.F.R.P bars have been evaluated the experimental value with 0.1mg precision. As per the standards, the H.F.R.P bars are weighed. Then, the H.F.R.P bar is immersed in distilled water at 230C and the wet weight of the bar is noted. The weight of the Sinker in immersed condition is also noted.

The laboratory tests carried out to evaluate the physical and mechanical properties of the newly developed H.F.R.P bars and are compared with that of conventional bars. The bond properties of H.F.R.P bars with concrete is also determined. Finally, it explains the experimental investigations on the flexural behavior of concrete one-way slabs reinforced with H.F.R.P reinforcements under static loading and are compared with conventional ones. The stress-strain performance of the sand-coated H.F.R.P bar is linear, lacking yield point up to the failure transverse shear strength is 3 times lesser than the tensile strength of the H.F.R.P bars. Thermal properties of fibers are substantially different in the longitudinal and transverse direction. Therefore the thermal characteristics vary between products according to the fiber, matrix and the fiber volume ratio. In this study the longitudinal Coefficient of linear thermal expansion is 7.5 x 10 -6/oC to 9x 10 -6/oC. Whereas the transverse Coefficient of linear thermal expansion is between 15 x 10 -6/oC to 20 x 10 -6/oC. Load - deflection graphs drawn exhibits the accordance between experimental and FEM (ANSYS) observations. The reduced deflection of FEM is due to the rigidness of meshing. The results also confer about the effect of tension stiffening and the bond slip. From the comparison it has been observed that experimental deflections vary from 1.03 to 1.37 times higher than the FEM deflections.

KEYWORDS: *H.F.R.P., Transverse Shear Strength, Flexural Behavior, FEM, Bond Properties, Compressive Strength*

How to cite this paper: Prerna Vaidya | Prof. Nitesh Kushwaha | Prof. Afzal Khan "An Analysis of Mechanical Properties and Flexural Behavior of Concrete Slabs Reinforced with H.F.R.P Reinforcements" Published in International Journal of Trend in Scientific Research and Development (ijtsrd), ISSN: 2456-6470, Volume-5 | Issue-3, April 2021, pp.98-111, URL: www.ijtsrd.com/papers/ijtsrd38691.pdf

IJTSRD38691

1. INTRODUCTION

In the era of concrete, concrete is exposed to chemical, such as carbonation and chloride adulteration break down the alkaline barrier in the cement. Subsequently, steel in the concrete becomes corrosive. Such phenomena lead to erosion of concrete at the reinforcement level, cracking and spelling of concrete due to volume increase of steel reinforcement. Different methods were investigated to overcome corrosion by numerous researchers. A possible solution to combat reinforcement corrosion for new construction is non-corrosive material for replacing steel. Light weight Eminent tensile strength and corrosion less characteristics make Fiber reinforced Polymer (F.R.P) suitable for such applications.

F.R.P in concrete has increased in recent time on account of resistance against corrosion, high tensile strength to weight ratio, and non-magnetization. The supremacy of the F.R.P materials, in comparison to normal building material such as steel bars, timber and RCC, lies in its improved strength and durability, stability, stiffness.

The main aspect of present research is to review the analytical and experimental behaviour of Hybrid Fiber Reinforced Polymer reinforcements F.R.P (HF.R.P) reinforcements in concrete one-way slabs on the basis of more accurate modeling and analysis and to build better recommendations for more balanced design. This chapter gives the development, constituents, classification, manufacturing methods and different applications of F.R.P materials. The manufacturing process of new H.F.R.P rod is also explained. Finally it presents need for present study and organization of the thesis.

2. METHODOLOGY

In laboratory tests carried out to evaluate the mechanical and physical properties of the newly developed H.F.R.P bars

and have a comparison with that of conventional bars. The manufacturing process of newly developed H.F.R.P bars are presented and secondly, the important properties such as Density, Tensile strength, Transverse shear, Coefficient of Thermal Expansion, and are determined according to ASTM standards and compared with that of conventional bars. The results shows good and satisfactory performance of H.F.R.P bars in comparison with Conventional bars. The bond performance of H.F.R.P rebars with concrete has also been examined. A detailed experimental procedure has been conducted to investigate the flexural behaviour of one-way slabs with all parametric conditions are presented.

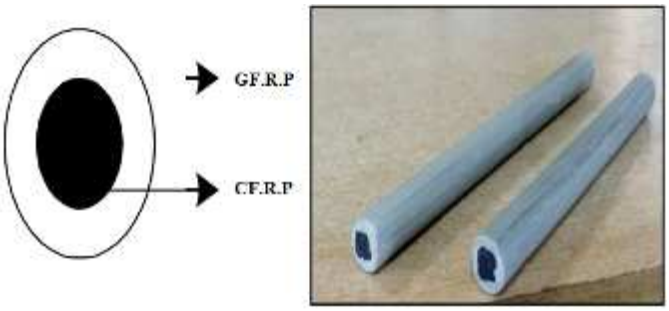

Figure 2.1 Cross Section View Of H.F.R.P Bar

3. RESULTS AND DISCUSSION

3.1. GENERAL

This chapter explains the laboratory tests carried out to evaluate the physical and mechanical properties of the newly developed H.F.R.P bars and are compared with that of conventional bars. The bond properties of H.F.R.P bars with concrete is also determined. Finally, it explains the experimental investigations on the flexural behaviour of concrete one-way slabs reinforced with H.F.R.P reinforcements under static loading and are compared with conventional ones.

3.2. Density

According to **ASTM D792-13** standards the density of H.F.R.P bars have been evaluated the experimental value with 0.1mg precision. As per the standards, the H.F.R.P bars are weighed at room temperature. Then, the H.F.R.P bar is immersed in distilled water at 23^{0}C and the wet weight of the bar is noted. The weight of the sinker in immersed condition is also noted. The specific gravity of H.F.R.P bars is calculated by using the

Specific gravity (23^{0}C) = a / (a +w -b) (Eqn3.1)
Density (23^{0}C) = specific gravity 23^{0}C×997.5 Kg/m^3(Eqn 3.2)

Where a is the apparent mass of specimen, before immersion in water sinker, b is the apparent mass of the specimen and the sinker immersed in water, w is the apparent mass of the immersed.

Table 3.1 presents the density of different H.F.R.P bars indicated in (ACI 440. 1R-15, 2015)

Type of Bar	Steel	GF.R.P	C.F.R.P	AF.R.P
Density (kg/m^3)	7900	1200–2100	1500–1600	1250–1400

Table 5.2 shows the density of new H.F.R.P bar of 10 mm diameter. It is seen that density increases with increasing fiber content. To determine the density, five H.F.R.P samples have been used and the density seems to be varied from 1961 kg/m^3 and 1988 kg/m^3 and it compared to conventional steel bars as 7850 kg/m^3.

Table 3.2 Density of H.F.R.P bars (present study)

Types of reinforcements	Density in *kg / m^3*
H1	1961
H2	1985
H3	1982
H4	1988
H5	1988
S	7850

Note: H- H.F.R.P bars, S-Steel bars

3.3. TENSILE TEST

The experimental results of tensile tests are shown in Table 5.3. All H.F.R.P specimens are failed in the gauge length due to rupture of fiber as shown in Fig 5.1 whereas, the conventional bars started yielding and then broken into two pieces.

Figure 3.1 Rupture of H.F.R.P bars

Table 3.3 Tensile properties of H.F.R.P and steel reinforcements

S. No	Specimen	Load	Tensile strength (MPa)	Elastic modulus (GPa)	Strain
1	H1	93.34	1189.04	49.5	0.023
2	H2	89.53	1145.69	50	0.025
3	H3	91.18	1161.52	51.5	0.028
4	H4	95.61	1217.93	50.5	0.027
5	H5	92.53	1178.72	52	0.028
6	S	45.5	590.60	200	0.003

Note: H- H.F.R.P bars, S-Steel bars

The Mean, Standard deviation and coefficient of variation for the tested specimens are calculated by using Eqn 3.3 to Eqn 3.5 respectively. The coefficient of variation values of H.F.R.P bars are less than 2% for their cases. Table 5.4 shows the statistical analysis of the tensile test.

The statistical analysis is shown in Table 5.4.

Table 3.4 Statistical analysis of the tensile test

Type of specimen	Mean	Standard deviation (MPa)	Coefficient of variation (%)
HF.R.P	1178.58	27.53	0.98

The experimental results indicated that the tensile strength of H.F.R.P bars is 1.5 to 2 times greater than steel bars whereas the tensile modulus which has been taken from the stress strain graph is found to be 4 times lesser than that of steel bars.

3.4. TRANSVERSE SHEAR STRENGTH

The shear strength of H.F.R.P bars is slightly higher than the conventional bars. The H.F.R.P bars posses three times lesser shear strength than its tensile strength. This is similar to conventional reinforcement and the shear strength has been evaluated using Eqn 3.6 and the results of the transverse shear test shown in Table 5.5.

$$\tau = \frac{p}{2A}$$

Table 3.5 Transverse shear strength of test specimens

Sl. No	Specimen	Area (mm^2)	Ultimate Load (kN)	Ultimate Shear strength (MPa)
1	H1	78.5	62.3	397.8
2	H2	78.5	64.2	409.2
3	H3	78.5	65.7	418.4
4	H4	78.5	61.4	391.6
5	H5	78.5	62.6	398.3
6	S	78.5	47.5	302.5

Note: H- H.F.R.P bars, S-Steel bars

3.5. COEFFICIENT OF THERMAL EXPANSION

Thermal properties of fibers are substantially different in the longitudinal and transverse direction. Therefore the thermal characteristics vary between products depending on the fiber matrix type and the fiber volume ratio. In this study the longitudinal Coefficient of linear thermal expansion is between 7.5 x 10^{-6}/°C to 9 x 10^{-6}/°C **(ACI 440. 1R-15, 2015)** whereas the transverse Coefficient of linear thermal expansion is between 15 x 10^{-6}/°C to 20 x 10^{-6}/°C.

Table 3.6 Coefficient of thermal expansion of reinforcements

Specimen	*L* (mm)	α ×10^{-6}/°C Longitudinal	α ×10^{-6}/°C Transverse
H1	50	7.5	15.1
H2	50	9	20
H3	50	7.5	15
H4	50	7.9	16.7
H5	50	8.3	18
S	50	12	12

Note: H- H.F.R.P bars, S-Steel bars

3.6. BOND MECHANISM

The bonding of concrete with reinforcing bars is the key to develop the composite action of RC elements. The properties of F.R.P bars are dissimilar to steel bars. At service loads, the tension stiffening effect of the concrete is affected by the F.R.P bars due to its difference local bond behavior which turn affects the cracking and deflection of RC member. Therefore, the bond test also has been carried out in the present study.

3.6.1. Modes of bond failure

Typical pullout mode of failures is occurred in all H.F.R.P specimens. In these HF.R.P-reinforced concrete cubes there are no visual cracks are noticed. It is observed that no damage at the loaded end for both concrete surface and bar where as at the free end, the surface layer of the bar is partly peeled off.

Figure 3.2 pullout test specimens

Figure 3.3 Bond Slip from Concrete and HF.R.P

Figure 3.4 Pullout failure

Figure 3.6 Failure pattern of HF.R.P bar in concrete

3.6.2. BOND STRESS-SLIP RESPONSES

In this test, a minimum bond stress and corresponding slip is noted at both the loaded and unloaded ends of all H.F.R.P specimens. At free ends, the slips are very smaller and it is about (0.08mm). At loaded ends, a slip of 3.60mm is reached at maximum bond stress. The bar slip of free ends are notably smaller than the loaded ends at all stages of loading. However, the high initial stiffness has been observed between H.F.R.P bar and concrete at loaded and unloaded ends. Experimental pullout results of H.F.R.P and Steel bars have shown in Table 5.7.

Table 3.7 Experimental pullout results of H.F.R.P and Steel bars

Types of Reinforce Ments	Rod diameter, d_b mm	Embedmen t Length, l_{bf}, mm	Compressive strength (MPa)	Pullout Load at failure,P (kN)	Bond Strength MPa
HF.R.P-1	10	60	49	41.56	13.23
HF.R.P-2	10	60	49	44.95	14.3
HF.R.P-3	10	60	49	36.12	11.5
HF.R.P-4	10	60	49	32.70	9.22
HF.R.P-5	10	60	49	41.24	13.10
STEEL-1	10	60	49	48.28	25.61
STEEL-2	10	60	49	37.18	19.71
STEEL-3	10	60	49	38.09	20.2
STEEL-4	10	60	49	45.52	24.15
STEEL-5	10	60	49	47.21	25.10

As given in the specifications of the ASTM D7913/D7913M-14, for each sequence of tests are calculated the average, Standard deviation and coefficient of variation and the COV of H.F.R.P specimens are less than 2% for these cases and by using the following equations 3.10 to 3.12. Table.5.8 shows the statistical analysis of the bond strength.

$\bar{x} = \sum^{s} x_i / n$ (Eqn.3.10)

$S_{n-1} = \sum_{i=1}^{n} x^2 - n\bar{x}^2)/(n-1)$ (Eqn.3.11)

$COV = 1 - (S_{n-1}/\bar{x})$ (Eqn.3.12)

Where $\bar{x}$ = mean; S_{n-1} = standard deviation; COV= coefficient of variation; n = number of tested specimens; x_1= measured or derived property. Table 5.8 shows of Statistical Analysis of the bond strength.

Table 3.8 Statistical Analysis of the bond strength

Type of specimen	Mean	Standard deviation (MPa)	Coefficient of variation (%)
HF.R.P	12.3	1.25	0.91
STEEL 10	22.95	0.40	0.95

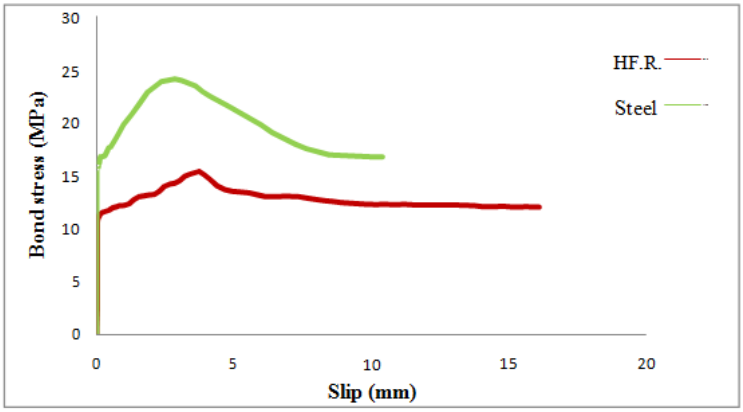

Figure 3.7 Bond Stress –Slip Of H.F.R.P And Conventional Steel Bars

Regarding the experimental observations, it is concluded that the bond strength of steel bars to concrete is superior to H.F.R.P bars nearly 1.8 times. The bond strength may be increased by increasing concrete strength and by decreasing the embedded length.

3.6.3. EXPERIMENTAL INVESTIGATIONS

Table 3.9 Experimental Results

Sl No	Designation of slabs	P_u (kN)	M_u, kNm	Ultimate Deflection (mm)
1	$m_1hp_1D_1$	40	16	97.63
2	$m_1hp_2D_1$	42.5	17	89.54
3	$m_1hp_3D_1$	45	18	80.44
4	$m_2hp_1D_1$	47.5	19	79.18
5	$m_2hp_2D_1$	50.25	20	77.72
6	$m_2hp_3D_1$	55	22	74.56
7	$m_1hp_1D_2$	57.5	23	70.80
8	$m_2hp_1D_2$	60	24	69.24
9	$m_3hp_1D_2$	75	30	58.45
10	$m_1sp_1D_1$	25	10	42.42
11	$m_1sp_2D_1$	27.5	11	40.71
12	$m_1sp_3D_1$	30	12	39.38
13	$m_2sp_1D_1$	27.5	11	36.75
14	$m_2sp_2D_1$	30	12	31.28
15	$m_2sp_3D_1$	32.5	13	30.12
16	$m_1sp_1D_2$	35	14	30.6
17	$m_2sp_1D_2$	30	12	30.55
18	$m_3sp_1D_2$	27.5	11	35.95

m_1, m_2, m_3 = Grades of concrete M30 ,M40 and M50 respectively; h_1,h_2,h_3 = Different reinforcement ratios 0.49%, 0.65% and 0.81% f H.F.R.P rebars respectively; s_1, s_2, s_3,= Different reinforcement ratios 0.49%, 0.65% and 0.81% f steel rebars respectively ;d_e = Effective depth of slab ;

M_u = Ultimate moment in kNm.

P_u = Static ultimate load in kN;

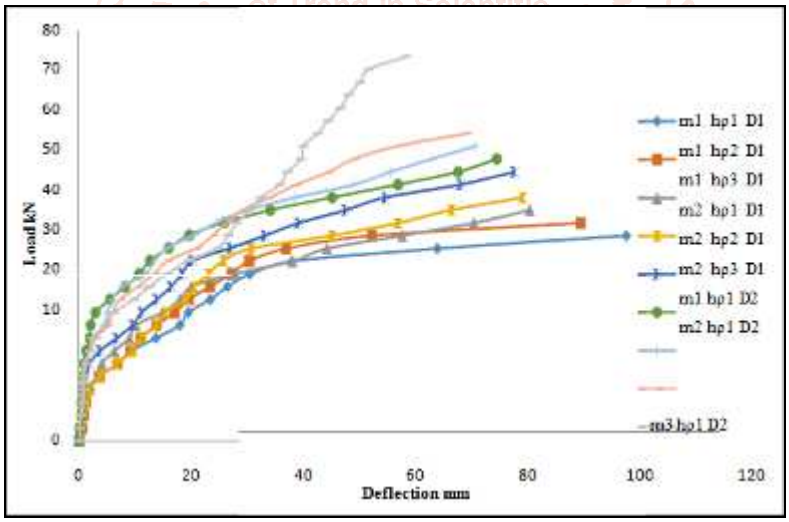

Figure 3.9 LOAD VS DEFLECTION for all H.F.R.P slabs

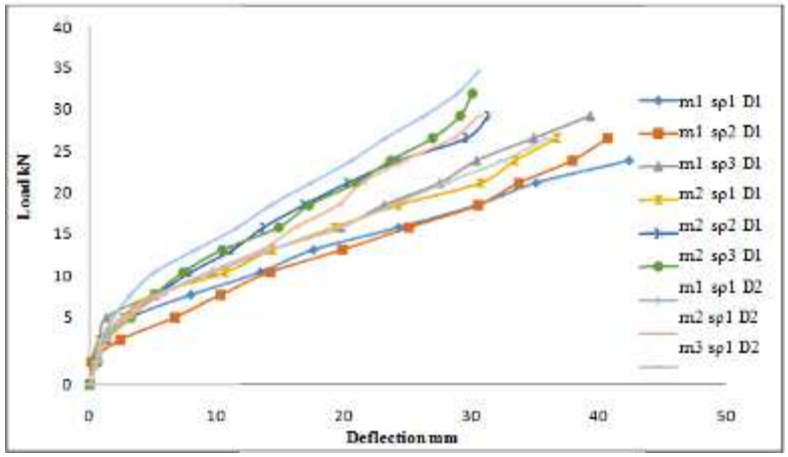

Figure 3.10 LOAD VS DEFLECTION for all conventional slabs

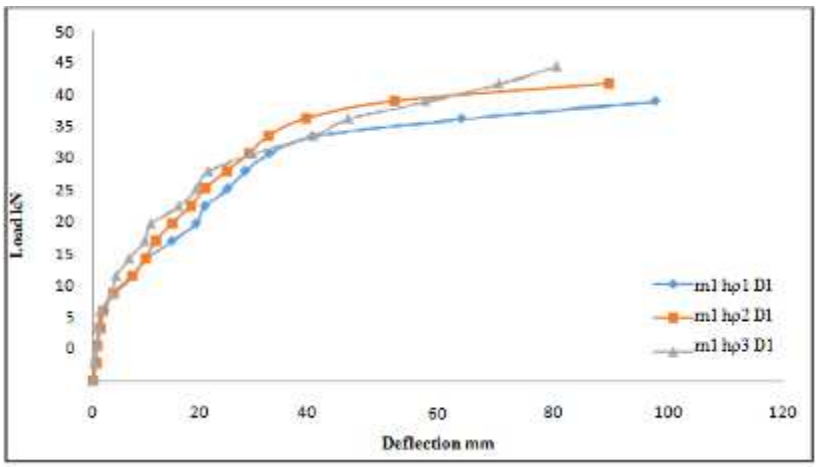

Figure 3.11 LOAD VS DEFLECTION H.F.R.P slabs for various reinforcement ratio.

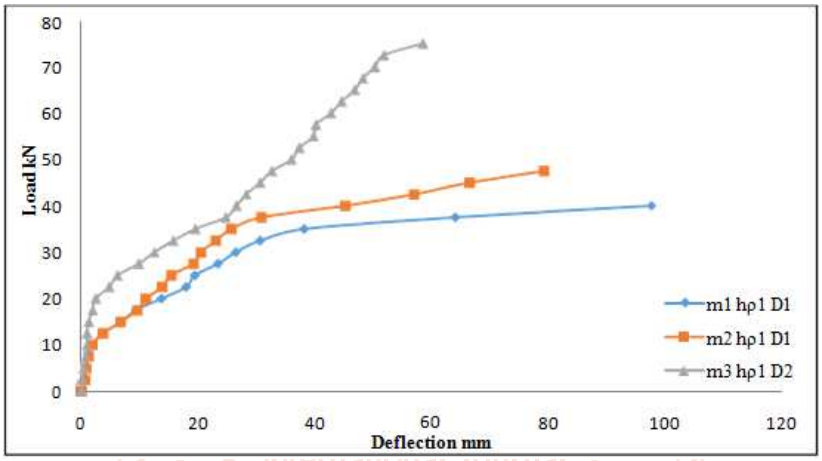

Figure 3.12 LOAD VS DEFLECTION for H.F.R.P slabs in various grade of concrete.

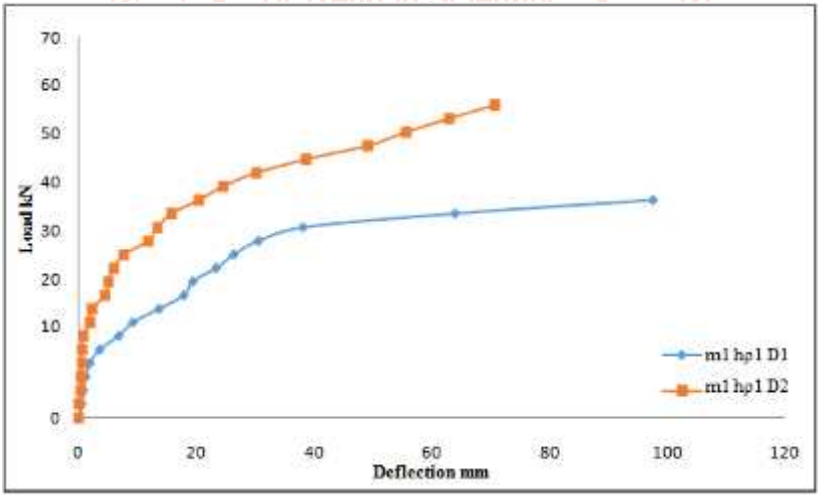

Figure 3.13 LOAD VS DEFLECTION for H.F.R.P slabs in various thickness.

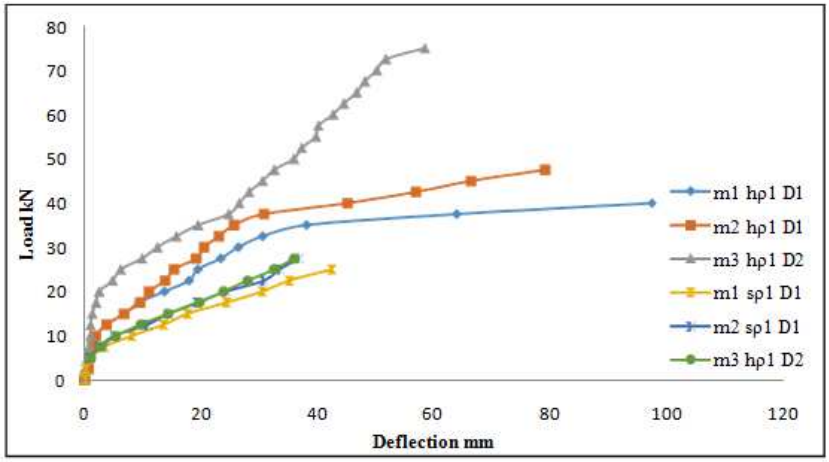

Figure 3.14 LOAD VS DEFLECTION for H.F.R.P and conventional slabs in different grade of concrete.

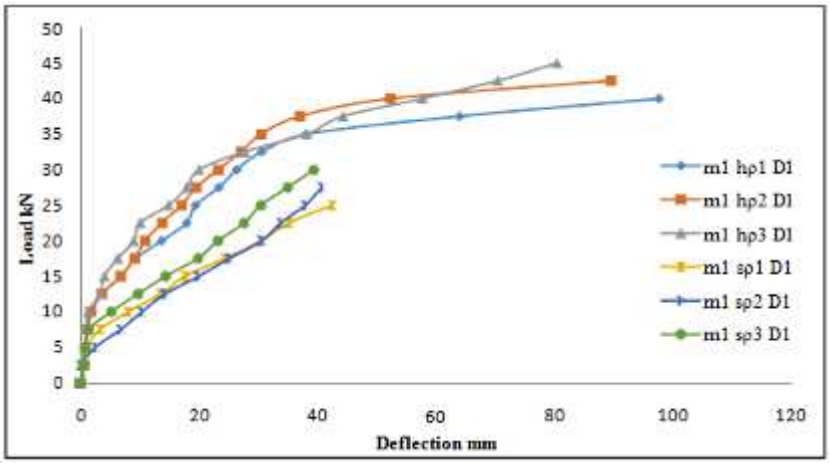

Figure 3.15 LOAD VS DEFLECTION for H.F.R.P and conventional slab of different reinforcement ratio.

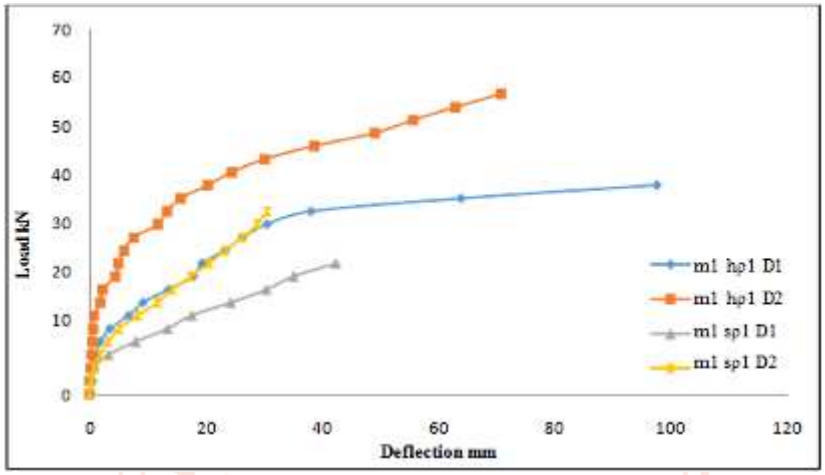

Figure 3.16 LOAD VS DEFLECTION for H.F.R.P and conventional slabs in different depths.

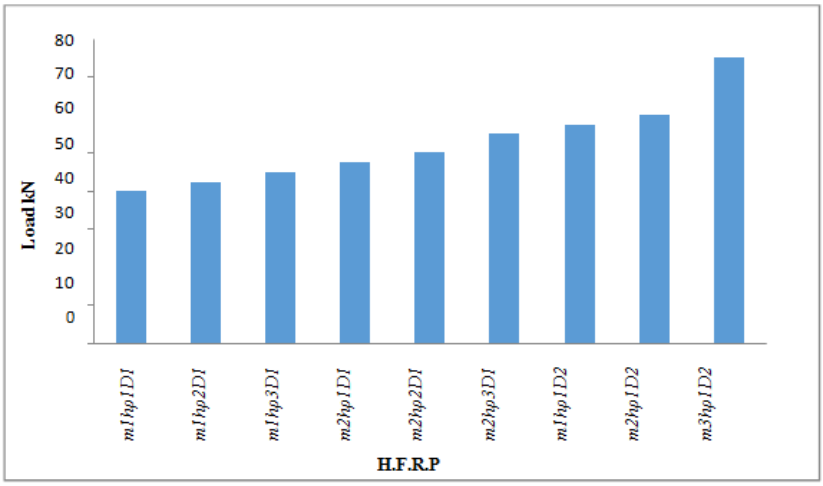

Figure 3.17 Bar Chart showing ultimate strength comparison of all H.F.R.P slabs

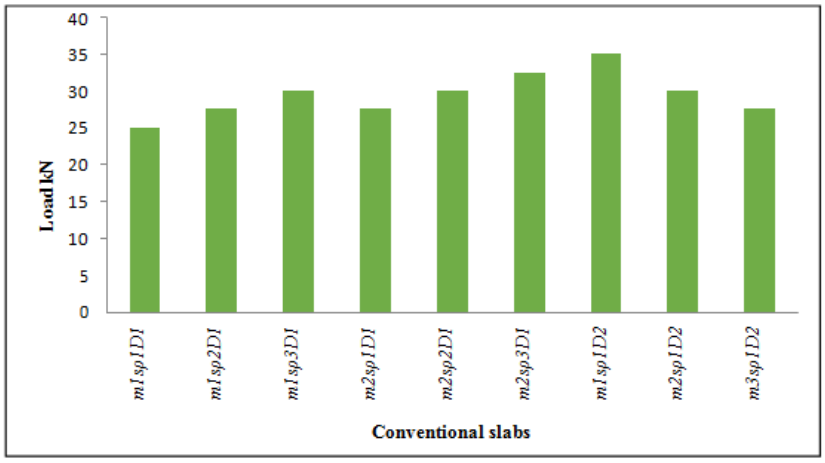

Figure 3.18 Bar Chart showing ultimate strength comparison of all steel slabs

Figure 3.19 Schematic diagram shows location of brass pellets

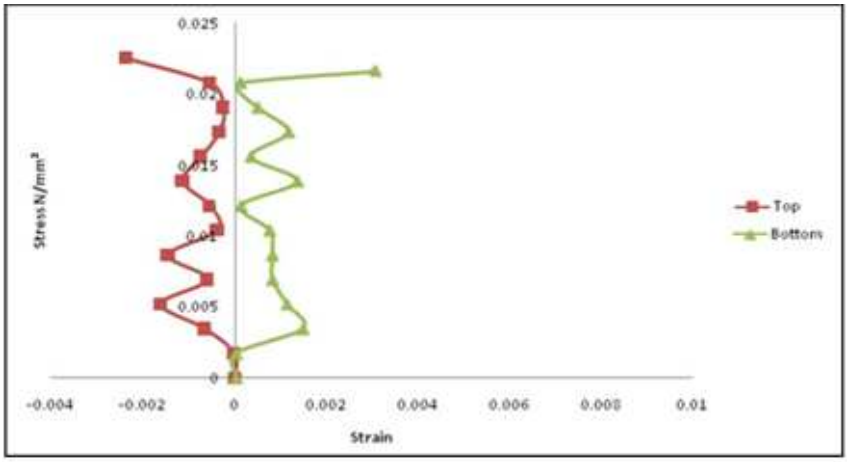

Figure 3.20 Comparison of stress versus strain for H.F.R.P slab for $m_1 h\rho_1 D_1$ at top and bottom levels

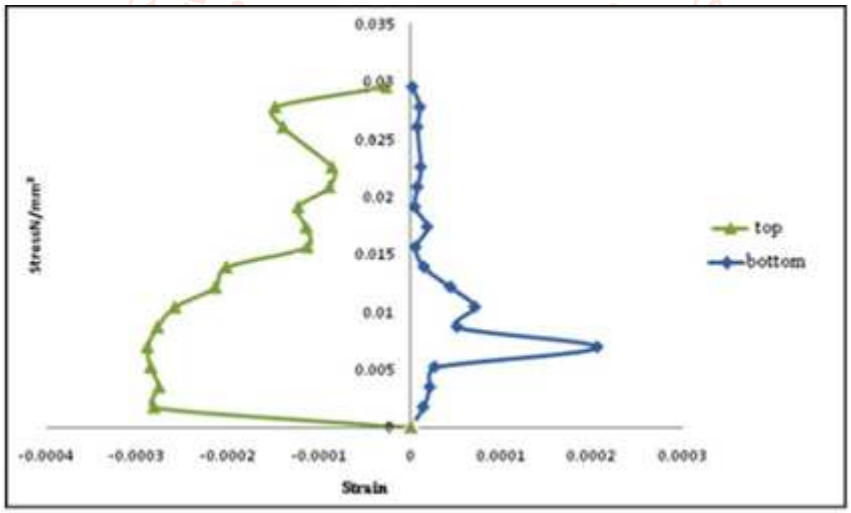

Figure 3.21 stress vs strain of Steel for $m_1 s\rho_1 D_1$ at top and bottom levels

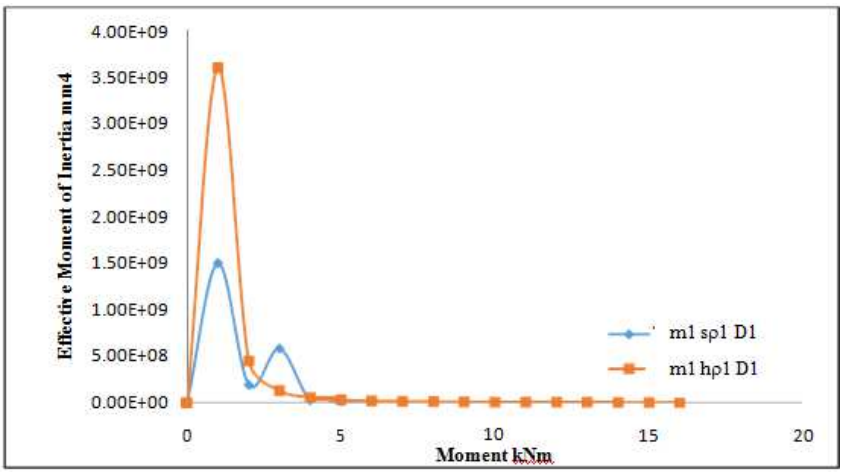

Figure 3.22 Effective Moment of Inertia versus Moment for H.F.R.P and conventional slabs

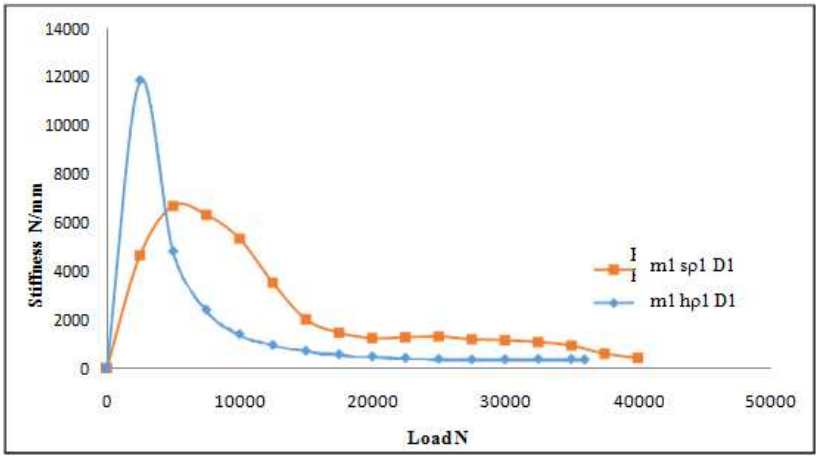

Figure 3.23 Stiffness versus Load for H.F.R.P and conventional slabs

Figure 3.24 Plane view

Figure 3.25 Different crack pattern of conventional slabs

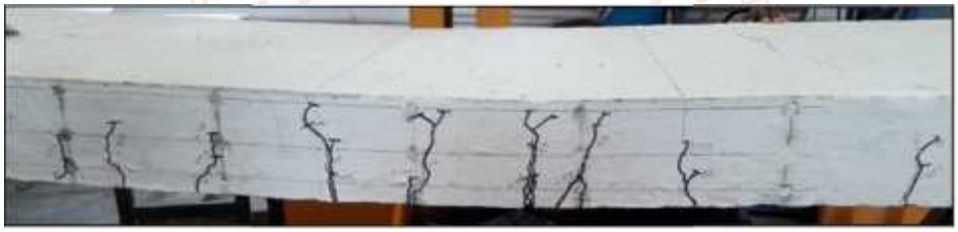

Figure 3.26 Section view

Figure 3.27 Different crack pattern of H.F.R.P slabs

Figure 3.28 Rupture of H.F.R.P $m_3hq_1D_2$ slabs

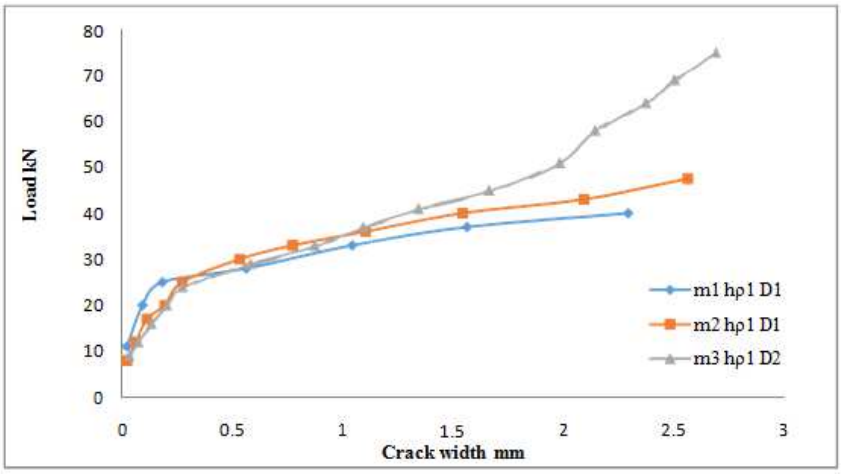

Figure 3.29 LOAD VS CRACK WIDTH for H.F.R.P slabs differing with grades of concrete.

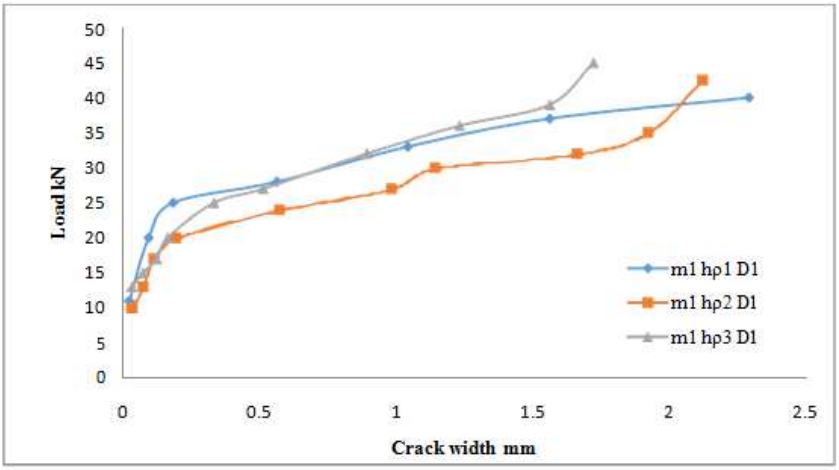

Figure 3.30 LOAD VS CRACK WIDTH of H.F.R.P slabs differing with reinforcement ratio

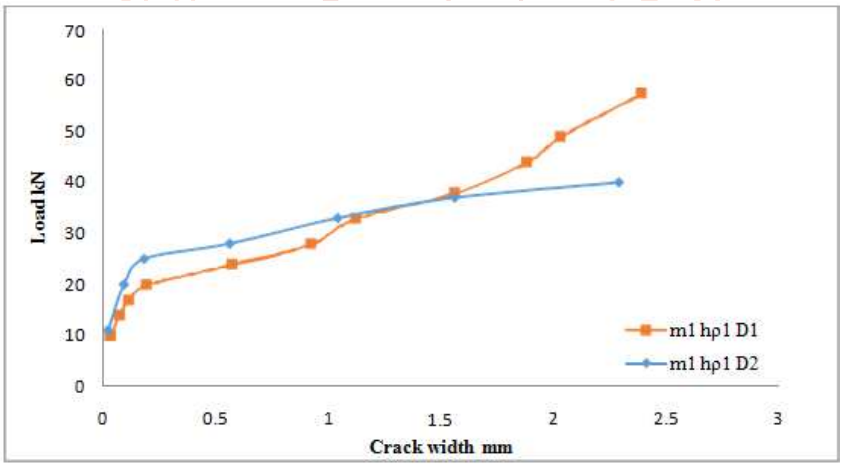

Figure 3.31 LOAD VS CRACK WIDTH of H.F.R.P slabs differing with depth of slabs

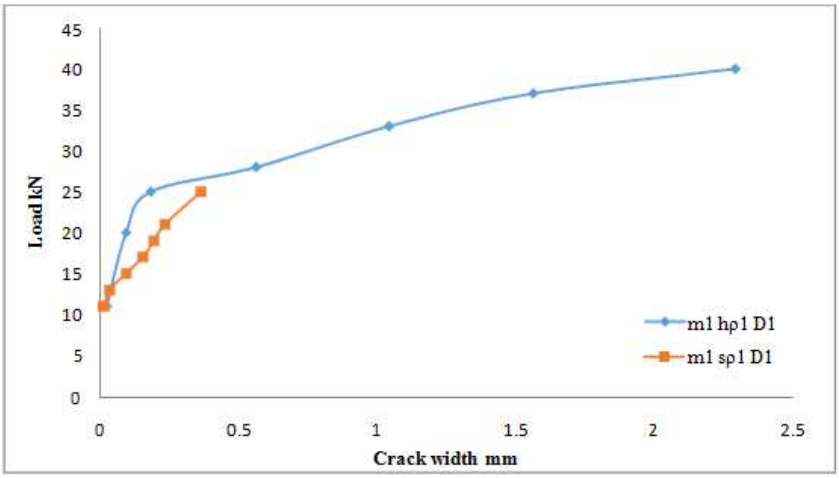

Figure 3.32 LOAD VS CRACK WIDTH between H.F.R.P slabs and conventional slabs

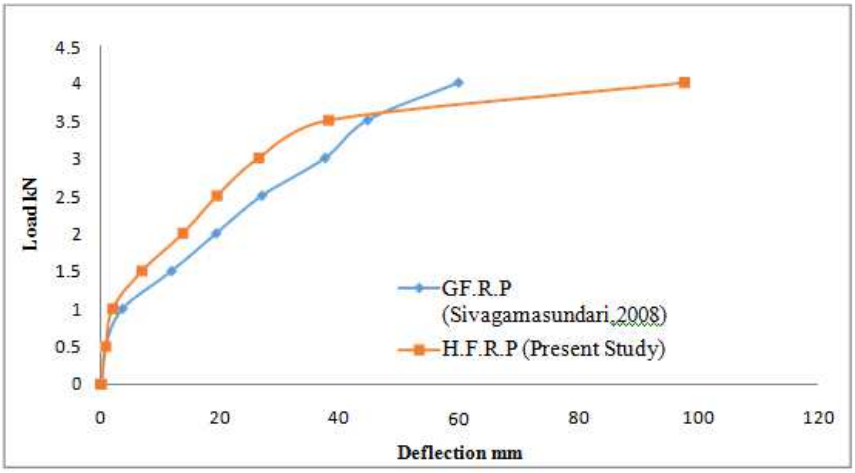

Figure 3.33 Comparison on LOAD VS CRACK WIDTH of between H.F.R.P slabs (present study) and G.F.R.P slabs

Regarding bond characteristics, it has seen that sand coating surface treatment on the rebars influences much on bond behavior lead for increase in chemical bond at early stages. However, once the peak strength has been reached, the sand coating surface debonds from the rebar and an abrupt decay of bond stresses occurs. The stress slip for sand coated H.F.R.P bar resembles conventional ones. Including micro slippage branch, a slippage branches, descending branch and a reduced branch at various load levels namely elastic, ultimate and residual levels. Regarding the experimental observations, it can be said that bond strength for steel bars to concrete is superior to H.F.R.P bars nearly 1.8 times. Bond strength can increase by increasing concrete strength and by decreasing the embedded length.

Table 3.10 an experimental Comparison between conventional and H.F.R.P slabs

SL NO	H.F.R.P SLABS	CONVENTIONAL SLABS	$\frac{M_{HF.R.P}}{M_{Steel}}$	$\frac{\delta_{HF.R.P}}{\delta_{Steel}}$	$\frac{w_{crH.F.R.P}}{w_{cr\ Steel}}$
1	$m_1hq_1D_1$	$m_1s_1D_1$	1.86	2.30	3.33
2	$m_1hq_2D_1$	$m_1s_2D_1$	1.83	2.20	2.94
3	$m_1hq_3D_1$	$m_1s_3D_1$	1.43	2.04	2.81
4	$m_2hq_1D_1$	$m_2s_1D_1$	1.90	2.15	2.73
5	$m_2hq_2D_1$	$m_2s_2D_1$	1.77	2.48	2.66
6	$m_2hq_3D_1$	$m_2s_3D_1$	1.95	2.43	2.43
7	$m_1hq_1D_2$	$m_1s_1D_2$	2.07	2.31	2.5
8	$m_2hq_1D_2$	$m_2s_1D_2$	2.22	2.26	2.14
9	$m_3hq_1D_2$	$m_3s_1D_2$	2.96	1.62	2.12

From the static test, it has seen that increase in the reinforcement ratio, grades of concrete and the thickness of the slab exhibit higher strength, less deflection and reduction in crack. some points can be observed from static flexural investigations of the slab.

1. Load deflection response due to static loading shows a greater reduction in stiffness in the case of H.F.R.P reinforced slabs than the conventional slabs. For conventional slabs, a wider deflection occurs due to its yielding nature, whereas H.F.R.P reinforced slabs show no yielding of reinforcements but a larger deflection occur due to load increments.
2. The flexural response of RC members is divided into two distinct stages. The first stage describes the uncracked portion of the member, and the second describes the cracked portion of the member.
3. In the second stage, the concrete tensile resistance reduces due to cracks and so that the tensile loads are carried entirely by the reinforcement. The flexural stiffness of a RC member is greatly reduced in this stage, but the cracked response remains well above that of a member that is fully cracked. This is possible only, due to good bonding and the by transferring mechanism of rebar, some of the tension to its surroundings, which leads to the contribution of concrete between individual cracks.
4. On further loading, the tensile stress increases to develop additional cracks. The process continues until crack spacing reduces in such a way not to develop new cracks. Such crack pattern is termed as the stabilized crack pattern in which additional load widens existing cracks, with limited effects on flexural stiffness.
5. The slab $m_1hq_1D_1$ shows 6.25 % increase in load carrying capacity than $m_1hq_2D_1$ slab whereas the deflection is 1.09 times greater $m_1hq_2D_1$ than slab. The slab $m_1hq_1D_1$ shows 12.5 % increase in load carrying capacity than $m_1hq_3D_1$ slab whereas the deflection is 1.21 times greater $m_1hq_2D_1$ than slab.
6. The load carrying capacity of H.F.R.P slab $m_1h\rho_1D_1$poses 6.25 % and 12.5 % decrease in load carrying capacities and times greater deflections than and $m_1h\rho_3D_1$ slabs.$m_1h\rho_2D_1$
7. By increasing the thickness by 20 mm the load carrying capacity increases by
8. 43.75 % and deflection reduces by 1.43 times.
9. By increasing the grades of concrete, $m_2h\rho_1D_1$shows 18.75 % and $m_3hq_1D_2$ shows 87.5% higher strengths and at the same time, and 1.8 times lesser deflections than $m_1h\rho_1D_1$slab .The experimental load deflection graphs are depicted from Fig.3.27 to 3.28. Owing to it, the ultimate deflection and the crack width also reduce substantially.

10. Fig.3.35 shows a comparative graph of ultimate strengths of all H.F.R.P slabs using bar chart. Similarly, Fig.3.36 shows a comparative graph of ultimate strengths of all conventional slabs using bar chart.
11. The strain distributions across the thickness of H.F.R.P slabs are shown in Fig.3.37 and Fig.3.38 H.F.R.P reinforcements in tension side of the concrete slabs behave similar to the H.F.R.P reinforcements tested under pure tension (Tensile test specimen) Reflecting good bonding between concrete and H.F.R.P reinforcements. The concrete surface strain in H.F.R.P reinforced slabs shuttles between 1.5 to 2 times greater than the conventional slabs under the similar load level. The experimental observations resembles to the observations made by the authors.
12. Experimental contributions on Crack widths and Crack patterns are shown from Fig.3.41 to Fig.3.43. The first crack appears at the middle of the slab and develops slowly across the width of the slab. When more loads is applied gradually, new cracks are developed on the slabs. At the same time, the existing crack has been widened. This is continued up to 75% of ultimate load and then the formation of new split up into smaller cracks close to the main bars. All the slabs experience flexural type of failure. At ultimate load, H.F.R.P reinforced slabs experience concrete crushing and Steel reinforced slabs show the flexural type of failure. Fig.3.41 and Fig.3.42 depict the crack pattern of slabs for various parameters.

3.7. DEFORMABILITY FACTORS

Ductility is the energy absorption capacity of a structure without failure and is to measure the inelastic deformation. For steel-reinforced structures, ductility is the ratio between the ultimate deformation and the deformation at yielding. This way of estimating ductility cannot be applied to F.R.P reinforced structures because they are virtually linear until failure.

Deformability factors quantify the safety of a HF.R.P-reinforced member similar to ductility factors in numerically. This factor, however, does not incorporate the advantageous post-yield behaviour of steel-reinforced flexural members. According to, a large curvature is needed for a higher moment of resistance. Thus, an accurate quantification of safety must account for load resistances (moments, forces, or stresses) as well as member deformations (curvature, displacement, or strains).

Deformability factors overcome this problem. A flexural member, properly designed with adequate deformability, can meet serviceability requirements, but still have enough reserve strength and deflection to allow pre-emptive warning of failure. Deformability factors account for this effect by comparing energy absorption at two different load levels i.e. energy absorbed at ultimate state with the energy absorbed at service load level. For the present study DF has been calculated from the experimental observations.

The Deformability Factor DF shown in Eqn 3.13 is obtained by multiplying the Moment factor by Curvature factor; accordingly,

DF = Moment factor × Curvature factor

The procedure is based on restriction of cracks widths at service load condition and ensuring that adequate deformability of the slab occurs before failure. By limiting the stress in the reinforcements it can be achieved. The stress in H.F.R.P reinforcements at service loads is depends on the ultimate strength of slab. Therefore the design requirement governs the amount of H.F.R.P reinforcement ratio provided. Based on this study, the deformability factor exceeds a value of 4 as specified in previous studies **(Newhook *et al.*, 2002, CEB-FIP, 2007; ACI 440. 1R-15, 2015)**. This study limits the strain in H.F.R.P ($\varepsilon_{H.F.R.P}$) due to service loads to 1.5 times the strain allowed for steel reinforcements (ε_y) which is equal to the strain 0.002 of slab.

Since F.R.P bars do not yield, a deformability factor is used and a minimum required value, DF=4, is proposed. The permissible value of strain in steel is limited to 0.002 as serviceability condition which is proposed to result in crack widths 5/3 times larger than the widths when steel bars are used. It is shown, by a parametric study, that when the F.R.P is determined in this way, the DF is commonly greater than 4; thus, there is no need to check the deformability.

Table 3.11 Deformability Factors For Concrete One-Way Slabs (Experimental Values)

Sl. No	Designation of slabs	$\rho_{HF.R.P}$ %	Serviceability condition		Ultimate condition		Deformability factor, DF
			M_s kNm	$\psi_s x10^{-5}$	M_u KNm	$\psi_u x10^{-5}$	
1	$m_1hq_1D_1$	0.49	1.4	6.25	19.7	31.25	69.1024
2	$m_1hq_2D_1$	0.65	1.8	6.25	26.3	31.25	69.4929
3	$m_1hq_3D_1$	0.81	2.3	6.25	32.9	31.25	69.7001
4	$m_2hq_1D_1$	0.49	1.6	6.25	19.8	31.25	68.1232
5	$m_2hq_2D_1$	0.65	1.9	6.25	26.4	31.25	68.3671
6	$m_2hq_3D_1$	0.81	2.4	6.25	33.0	31.25	68.5426
7	$m_1hq_1D_2$	0.39	1.7	5	24.70	25.13	69.4586
8	$m_2hq_1D_2$	0.39	1.8	5	24.8	25.13	67.2455
9	$m_3hq_1D_2$	0.39	1.8	5	24.9	25.13	66.1958
10	$m_1sq_1D_1$	0.49	3.1	5.85	17.8	73.75	3.567468
11	$m_1sq_2D_1$	0.65	4.3	5.85	11.7	73.75	3.579506
12	$m_1sq_3D_1$	0.81	5.1	5.85	14.6	73.75	3.598571
13	$m_2sq_1D_1$	0.49	3.1	5.85	17.8	73.75	3.567468
14	$m_2sq_2D_1$	0.65	4.3	5.85	11.7	73.75	3.579506
15	$m_2sq_3D_1$	0.81	5.1	5.85	14.6	73.75	3.598571
16	$m_1sq_1D_2$	0.39	3.8	4.69	10.98	59.63	3.579793
17	$m_2sq_1D_2$	0.39	3.8	4.69	10.9	59.63	3.579793
18	$m_3sq_1D_2$	0.39	3.8	4.69	10.9	59.63	3.579793

The procedure is based on restriction of cracks widths at service load condition. Therefore the design H.F.R.P reinforcement ratio provided. Based on this study, the deformability factor exceeds a value of 4 as specified in previous studies. This study limits the strain in H.F.R.P ($\varepsilon_{H.F.R.P}$) due to service loads to 1.5 times the strain allowed for steel reinforcements (ε_y) which is equal to the strain 0.002 of slab.

Since F.R.P bars do not yield, a deformability factor is used and a minimum required value, DF=4, is proposed. The permissible value of strain in steel is limited to 0.002 as serviceability condition which is proposed to result in crack widths 5/3 times larger than the widths when steel bars are used. It is shown, by a parametric study, that when the F.R.P is determined in this way, the DF is commonly greater than 4; thus, there is no need to check the deformability.

4. CONCLUSIONS

4.1. GENERAL

In this Chapter, the essential contributions of this study are summarized .Finally the suggestions for further researches are also presented.

4.1.1. SALIENT CONCLUSIONS OF THE PRESENT STUDY

The stress-strain performance of the sand-coated H.F.R.P bar is linear, lacking yield point up to the failure transverse shear strength is 3 times lesser than the tensile strength of the H.F.R.P bars. Thermal properties of fibers are substantially different in the longitudinal and transverse direction. Therefore the thermal characteristics vary between products according to the fiber, matrix and the fiber volume ratio. In this study the longitudinal Coefficient of linear thermal expansion is 7.5 x 10 $^{-6/o}$C to 9x 10 $^{-6/o}$C. Whereas the transverse Coefficient of linear thermal expansion is between 15 x 10 $^{-6/o}$C to 20 x 10 $^{-6/o}$C. Load –deflection graphs drawn exhibits the accordance between experimental and FEM (ANSYS) observations. The reduced deflection of FEM is due to the rigidness of meshing. The results also confer about the effect of tension stiffening and the bond slip. From the comparison it has been observed that experimental deflections vary from 1.03 to 1.37 times higher than the FEM deflections.

4.2. FUTURE SCOPE OF WORK

- The long-term properties of H.F.R.P reinforcements under different exposure conditions with different types of fibers and matrix composition needs to be assessed by rigorous experimental study.
- Application of rigorous reliability studies incorporating the experimental observations can be extended to H.F.R.P reinforced concrete columns, beam-column connections, beams under tensional loading conditions, etc.
- Investigations on the fatigue characteristics of H.F.R.P reinforced concrete slabs need to be experimented.
- The finite element study on the non linear aspects of the behaviour of H.F.R.P reinforced concrete slabs needs to be studied under repeated loading conditions.

REFERENCES

[1] ACI 544.3R-93: Guide for Specifying, Proportioning, Mixing, Placing, and Finishing Steel Fiber Reinforced Concrete, American Concrete Institute, 1998

[2] ASTM C1116/C1116M – 06

[3] "AROVEX™ Nanotube Enhanced Epoxy Resin Carbon Fiber Prepreg – Material Safety Data Sheet" (PDF). Zyvex Performance Materials. 8 April 2009. Archived from the original (PDF) on 16 October 2012. Retrieved 26 March 2015.

[4] ACI-318-IBC-IRC-Evaluation-report-Helix-Steel-Micro-Rebar-Alternative-to-Steel-Rebar-Concrete-reinforcement-Vertical-Applications.pdf

[5] Almudaihesh, Faisel; Holford, Karen; Pullin, Rhys; Eaton, Mark (1 February 2020). "The influence of water absorption on unidirectional and 2D woven CFRP composites and their mechanical performance". Composites Part B: Engineering. **182**: 107626. doi:10.1016/j.compositesb.2019.107626. ISS N 1359-8368.

[6] "AERO – Boeing 787 from the Ground Up". Boeing. 2006. Archived from the original on 21 February 2015. Retrieved 7 February 2015

[7] "Busted Carbon". Archived from the original on 30 November 2016. Retrieved 30 November 2016.

[8] "Carbon Technology". Look Cycle. Archived from the original on 30 November 2016. Retrieved 30 November 2016.

[9] "Carbon fibre reinforced plastic bogies on test". Railway Gazette. 7 August 2016. Archived from the original on 8 August 2016. Retrieved 9 August 2016.

[10] Corum, J. M.; Battiste, R. L.; Liu, K. C; Ruggles, M. B. (February 2000). "Basic Properties of Reference Crossply Carbon-Fiber Composite, ORNL/TM-2000/29, Pub57518" (PDF). Oak Ridge National Laboratory. Archived (PDF) from the original on 27 December 2016.

[11] "Engines". Flight International. 26 September 1968. Archived from the original on 14 August 2014.

[12] FIRE PROTECTION OF CONCRETE TUNNEL LININGS by Peter Shuttle worth, Rail Link Engineering. UK

[13] Guzman, Enrique; Cugnoni, Joël; Gmür, Thomas (May 2014). "Multi-factorial models of a carbon fibre/epoxy composite subjected to accelerated environmental ageing". Composite Structures. **111**: 179–192. doi:10.1016/j.compstruct.2013.12.028

[14] Guzman, Enrique; Gmür, Thomas (dir.) (2014). "A Novel Structural Health Monitoring Method for Full-Scale CFRP Structures" (PDF). EPFL PhD thesis. doi:10.5075/epfl-thesis-6422. Archived (PDF) from the original on 25 June 2016.

[15] Henry, Alan (1999). McLaren: Formula 1 Racing Team. Haynes. ISBN 1-85960-425-0.

[16] Howard, Bill (30 July 2013). "BMW i3: Cheap, mass-produced carbon fiber cars finally come of age". Extreme Tech. Archived from the original on 31 July 2015. Retrieved 31 July 2015.

[17] Hans, Kreis (2 July 2014). "Carbon woven fabrics". compositesplaza.com. Archived from the original on 2 July 2018. Retrieved 2 January 2018.

[18] "How is it Made". Zoltek. Archived from the original on 19 March 2015. Retrieved 26 March 2015.

[19] "ICC and Kookaburra Agree to Withdrawal of Carbon Bat". NetComposites. 19 February 2006. Retrieved 1 October 2018.

[20] Ismail, N. "Strengthening of bridges using CFRP composites." najif.net.

[21] Jump up to:[a b c] Courtney, Thomas (2000). Mechanical Behavior of Materials. United States of America: Waveland Press, Inc. pp. 247–249. ISBN 1-57766-425-6.

[22] Jump up to:[a b c d e f] Chawla, Krishan (2013). Composite Materials. United States of America: Springer. ISBN 978-0-387-74364-6.

[23] Kopeliovich, Dmitri. "Carbon Fiber Reinforced Polymer Composites". Archived from the original on 14 May 2012. substech.com

[24] Li, V.; Yang, E.; Li, M. (28 January 2008), Field Demonstration of Durable Link Slabs for Jointless Bridge Decks Based on Strain-Hardening Cementitious Composites – Phase 3: Shrinkage Control (PDF), Michigan Department of Transportation

[25] L:aChance, David (April 2007). "Reinventing the Wheel Leave it to Citroën to bring the world's first resin wheels to market". Hemmings. Archived from the original on 6 September 2015. Retrieved 14 October 2015.

[26] Lomov, Stepan V.; Gorbatikh, Larissa; Kotanjac, Željko; Koissin, Vitaly; Houlle, Matthieu; Rochez, Olivier; Karahan, Mehmet; Mezzo, Luca; Verpoest, Ignaas (February 2011). "Compressibility of carbon woven fabrics with carbon nanotubes/nanofibres grown on the fibres". Composites Science and Technology. **71** (3): 315– 325. doi:10.1016/j.compscitech.2010.11.024.

[27] Mechanical Properties of Recycled PET Fibers in Concrete, Materials Research. 2012; 15(4): 679-686

[28] "News - Fibres add much needed protection to prestigious tunnelling projects". 2007-09-27. Archived from the original on 2007-09-27. Retrieved 2017-02-05.

[29] Nguyen, Dinh; Abdullah, Mohammad Sayem Bin; Khawarizmi, Ryan; Kim, Dave; Kwon, Patrick (2020). "The effect of fiber orientation on tool wear in edge-trimming of carbon fiber reinforced plastics (CFRP) laminates". Wear. Elsevier B.V. 450–451: 203213. doi:10.1016/j.wear.2020.203213. ISSN 0043-1648.

[30] Ochia, T.; Okubob, S.; Fukuib, K. (July 2007). "Development of recycled PET fiber and its application as concrete-reinforcing fiber". Cement and Concrete Composites. **29** (6): 448–455. doi:10.1016/j.cemconcomp.2007.02.002.

[31] Pora, Jérôme (2001). "Composite Materials in the Airbus A380 – From History to Future" (PDF). Airbus. Archived (PDF) from the original on 6 February 2015. Retrieved 7 February 2015.

[32] Pike, Carolyn M.; Grabner, Chad P.; Harkins, Amy B. (4 May 2009). "Fabrication of Amperometric Electrodes". Journal of Visualized Experiments (27). doi:10.3791/1040. PMC 2762914. PMID 19415069.

[33] Petrány, Máté (17 March 2014). "Michelin Made Carbon Fiber Wheels For Citroën Back In 1971". Jalopnik. Archived from the original on 18 May 2015. Retrieved 31 July 2015.

[34] "Polyamid CF Filament - 3D Druck mit EVO-tech 3D Druckern" [Polyamide CF Filament - 3D printing with EVO-tech 3D printers] (in German). Austria: EVO-tech. Retrieved 4 June2019.

[35] Pozegic, T. R.; Jayawardena, K. D. G. I.; Chen, J-S.; Anguita, J. V.; Ballocchi, P.; Stolojan, V.; Silva, S. R. P.; Hamerton, I. (1 November 2016). "Development of sizing-free multi-functional carbon fibre nanocomposites". Composites Part A: Applied Science and Manufacturing. **90**: 306–319. doi:10.1016/j.compositesa.2016.07.012. ISSN 1359-835X.

[36] "Red Bull's How to Make An F1 Car Series Explains Carbon Fiber Use: Video". motorauthority. Archived from the original on 29 September 2013. Retrieved 11 October2013.

[37] Rahman, S. (November 2008). "Don't Stress Over Prestressed Concrete Cylinder Pipe Failures". Opflow Magazine. **34** (11): 10–15. doi:10.1002/j.1551-8701.2008.tb02004.x. Archived from the original on 2 April 2015.

[38] Ray, B. C. (1 June 2006). "Temperature effect during humid ageing on interfaces of glass and carbon fibers reinforced epoxy composites". Journal of Colloid and Interface Science. **298** (1): 111–117. Bibcode: 2006JCIS..298.111R. doi:10.1016/j.jcis.2005.12.023. PMID 16386268.

[39] Scott, Alwyn (25 July 2015). "Boeing looks at pricey titanium in bid to stem 787 losses". www.stltoday.com. Reuters. Archived from the original on 17 November 2017. Retrieved 25 July 2015.

[40] "Taking the lead: A350XWB presentation" (PDF). EADS. December 2006. Archived from the original on 27 March 2009.

[41] "The Perils of Progress". Bicycling Magazine. 16 January 2012. Archived from the original on 23 January 2013. Retrieved 16 February 2013.

[42] Thomas, Daniel J. (1 September 2020). "Developing hybrid carbon nanotube- and graphene-enhanced nanocomposite resins for the space launch system". The International Journal of Advanced Manufacturing Technology. **110** (7): 2249–2255. doi:10.1007/s00170-020-06038-7. ISSN 1433-3015.

[43] Trimble, Stephen (26 May 2011). "Lockheed Martin reveals F-35 to feature nanocomposite structures". Flight International. Archived from the original on 30 May 2011. Retrieved 26 March 2015.

[44] "Zyvex Performance Materials Launch Line of Nano-Enhanced Adhesives that Add Strength, Cut Costs" (PDF) (Press release). Zyvex Performance Materials. 9 October 2009. Archived from the original (PDF) on 16 October 2012. Retrieved 26 March 2015.

[45] Zhao, Z.; Gou, J. (2009). "Improved fire retardancy of thermoset composites modified with carbon nanofibers". Sci. Technol. Adv. Mater. **10** (1): 015005. Bibcode:2009STAdM..10a5005Z. doi:10.1088/14686996/10/1/015005. PMC 5109595. PMID 27877268.